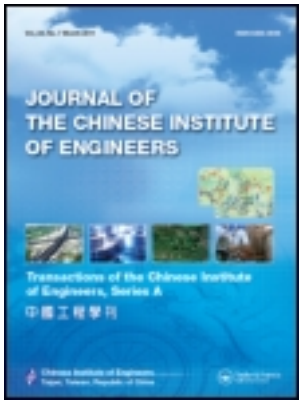

Journal of the Chinese Institute of Engineers
Publication details, including instructions for authors and subscription information:
http://www.tandfonline.com/loi/tcie20

Investigating mechanical properties of epoxy/organoclay nanocomposites

Jia-Lin Tsai [a] & Shin-Ming Hsu [b]

[a] Department of Mechanical Engineering , National Chiao Tung University , Hsinchu, Taiwan 300, R.O.C. Phone: 886-3-5731608 Fax: 886-3-5731608 E-mail:

[b] Department of Mechanical Engineering , National Chiao Tung University , Hsinchu, Taiwan 300, R.O.C.

Published online: 04 Mar 2011.

To cite this article: Jia-Lin Tsai & Shin-Ming Hsu (2008) Investigating mechanical properties of epoxy/organoclay nanocomposites, Journal of the Chinese Institute of Engineers, 31:1, 9-16, DOI: 10.1080/02533839.2008.9671355

To link to this article: http://dx.doi.org/10.1080/02533839.2008.9671355

INVESTIGATING MECHANICAL PROPERTIES OF EPOXY/ ORGANOCLAY NANOCOMPOSITES

Jia-Lin Tsai* and Shin-Ming Hsu

ABSTRACT

This study aims to investigate the organoclay effect on the mechanical properties of epoxy nanocomposites. In order to characterize the organoclay effect, three different loadings of organoclay, 2.5, 5, and 7.5 wt%, were dispersed into the epoxy with a mechanical blender followed by sonication. Tensile tests and fracture tests were carried out on these specimens to determine their stiffness, strength and fracture behaviors. The experimental results obtained from tensile tests indicate that the stiffness of the epoxy increases with the increment of organoclay inclusion; however, the corresponding failure strain decreases. On the other hand, fracture tests on single-edge-notch bending specimens reveal that the inclusion of organoclay may dramatically reduce the fracture toughness of nanocomposites. The decrease could be due to changes in the morphologies of the epoxy nanocomposites as well as the interfacial debonding between the organoclay and the surrounding epoxy.

Key Words: organoclay, nanocomposites, fracture toughness, tensile strength.

I. INTRODUCTION

Nano-materials, such as carbon nanotubes, nano wires, organoclay etc., with superior mechanical behavior and higher aspect ratios have been considered as supreme reinforcements in composites (Thostenson *et al*., 2005; Pinnavaia and Beall, 2000; LeBaron *et al*., 1999). Composites reinforced with organoclay platelets are one particular class of nanocomposites and have attracted substantial attention since Toyota researchers successfully enhanced the mechanical properties of nylon6 a decade ago (Usuki *et al*., 1993a; Usuki *et al*., 1993b) The organoclay platelet is an ultra thin (1 nm) silicate film with lateral dimensions up to 1 μm. Without special processing, the platelets are held together by the weak ionic bond into clay clusters (tactoids). Through the ion exchange process, sodium ions attracted to the surfaces of the platelets are replaced by organic cations which may improve the interfacial adhesion between the polymer and the platelet and facilitate the exfoliation of the organoclay within the monomer. After an appropriate polymerization process, the aggregated platelets are exfoliated and dispersed uniformly in the polymer. Depending on the degree of exfoliation of the organoclay, three categories of nanocomposites, i.e., tactoids, intercalated and exfoliated, may be produced (Dennis *et al*., 2001). For tactoids, the clay platelets still aggregate together, and no polymer molecule moves into the galleries of the adjacent platelets. For intercalated nanocomposites, one or some molecular layers of polymer are inserted into the galleries of the platelets, and gallery spacing becomes 2-3 nm. When more polymer molecules move into the galleries resulting in the further separation of platelets, exfoliated nanocomposites are generated. In this case, gallery spacing is around 8 nm or more. The main goal of the fabrication process is to achieve exfoliated organoclay nanocomposites since experimental observations show that the stiffness of the nanocomposites can be enhanced if the platelets are well dispersed and that little improvement will be obtained if the platelets are lumped together (Cho and Paul, 2001; Okada and Usuki, 1995)

On the other hand, regarding fracture behavior as well as the fracture toughness of organoclay nanocomposites, no consistent results have been obtained so far. Some results indicate that the fracture

*Corresponding author. (Tel: 886-3-5731608; Fax: 886-3-5720634; Email: jialin@mail.nctu.edu.tw)

The authors are with the Department of Mechanical Engineering, National Chiao Tung University, Hsinchu, Taiwan 300, R.O.C.

toughness of the polymers rise with the increase of organoclay contents (Liu *et al*., 2004a; Liu *et al*., 2004b; Zerda and Lesser, 2001; Miyagawa and Drzal, 2003; Wang *et al*., 2004). Nevertheless, some adverse influences on fracture toughness are reported in the literature (Gam *et al*., 2003; Lu *et al*., 2002; Nair *et al*., 2002). This discrepancy could be due to varying organoclay morphology within the polymer caused by different methods of fabrication processing. The addition of nanoclay platelets, if not well exfoliated, may create weak spots which are prone to reduce fracture toughness. In view of the foregoing, although lots of studies regarding organoclay nanocomposites have been reported, the effect of organoclay on fracture toughness is still undefined. Therefore, it is necessary to perform a comprehensive investigation on this issue from the fabrication process to the morphology of the nanocomposites.

In this study, the degrees of exfoliation of the organoclay in nanocomposites were characterized using X-ray diffraction (XRD) and transmission electron microscopy (TEM). By means of three-point-bending Mode I fracture tests, the fracture toughness of the nanocomposites associated with three different organoclay loadings, 2.5, 5 and 7.5 wt%, were measured. The fracture surfaces around the crack tip were examined using optical microscopy and scanning electron microscopy (SEM) to determine the failure mechanism. Based on micrographic observations, the influences of the organoclay on the fracture behaviors of the nanocomposites are discussed.

II. PREPARATION OF ORGANOCLAY/ EPOXY NANOCOMPOSITE

The epoxy resin used in this study is diglycidyl ether of bisphenol A (DGEBA, EPON828 with an epoxy equivalent weight of 187) supplied by Resolution Performance Products. The curing agent is a polyoxypropylenediamine (Jeffamine D-230 with equivalent weight with epoxy of 60) provided by Huntsman Corp. The clay used for the synthesis of nanocomposites is organoclay (Nanomer I.30E) obtained from Nanocor Inc., which is basically a montmorillonite mineral, the surface of which is modified by octadecyl-ammonium ions, designed to be easily dispersed into amine-cured epoxy resin and to form nanocomposites (Technical data sheet). In preparation of the epoxy/clay nanocomposite samples, the organoclay clay was dried in the vacuum oven for 6 hours at 90°C in order to remove moisture and then blended with EPON828 at 80°C for 4 hours using a mechanical stirrer. The mixture was then sonicated (ultrasonic liquid processing) using a sonicator with a cooling system around the sample container until the compounds became transparent. In the liquid compound, microscopic bubbles are formed momentarily and then imploded by ultrasonic vibration. The collapse of the thousands of bubbles can cause powerful shock waves to radiate throughout the sample resulting in clay platelet separation. The epoxy/clay mixture was degassed at room temperature in a vacuum oven for 10 minutes and mixed with a curing agent (32 wt% of EPON828). The mechanical stirrer was again utilized to blend the final mixture at room temperature for 10 minutes. To form the nanocomposite specimens for tensile tests, the mixture was poured into a specially designed steel mold with Teflon-coated surfaces. Subsequently, the samples were cured at 100°C for 3 hours with an additional 3 hours at 125°C for post-curing. For the study, nanocomposites containing 2.5%, 5%, and 7.5% loadings (by weight) of organoclay were prepared, respectively. It is noted that when nanocomposites contain high organoclay loading, the viscosity becomes higher and retards the degassing process. More degassing time is required to effectively eliminate the embedded bubbles.

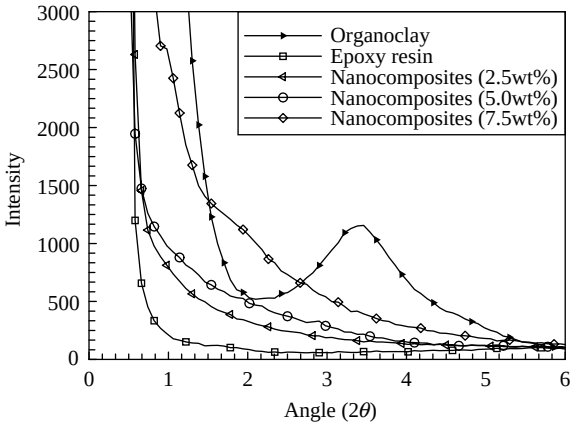

Fig. 1 X-ray diffractions of organoclay, neat epoxy and nanocomposites

III. CHARACTERIZATION OF EPOXY/ ORGANOCLAY NANOCOMPOSITES

In order to evaluate the degree of exfoliation of the organoclay in the epoxy resin, the samples were examined using XRD and TEM, both of which are widespread methods for characterizing the morphology of nanocomposites. XRD measurements were conducted on neat epoxy and epoxy/clay nanocomposite films (about 4mm thick) using a Bede D1 diffractometer. The incident X-ray wavelength was 1.54Å, and the scanning step size was 0.08 degree. Fig. 1 shows the XRD patterns for the nanocomposites containing various loadings of organoclay as well as the organoclay and pure epoxy resin. For organoclay, the reflection peak is detected at $2\theta = 3.78°$ corresponding to the 2.3 nm

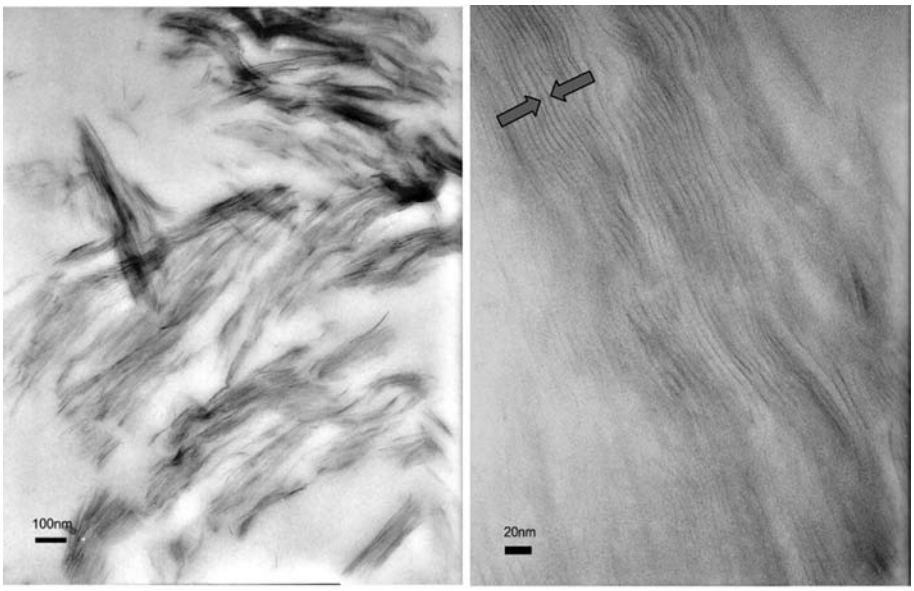

(a) (b)

Fig. 2 TEM micro-photos for the epoxy/organoclay nanocomposites ((a) 50,000 magnification; (b) 200,000 magnification)

interlayer spacing (d-spacing). However, there is no significant peak value found in the nanocomposites, which may be attributed to the fact that some clay platelets may not exhibit significant basal reflection or intensity pattern, nor are their relative peaks easily detected (Liu *et al*., 2004b). Thus, the XRD pattern may not be a full indication of the morphology of the nanocomposites.

To further understand the morphology of the nanocomposites, we utilized the TEM which can provide direct visualization of the spatial distribution of the organoclay. Thin film samples of epoxy/organoclay nanocomposites with 5 wt% organoclay (about 100 nm thick) were cut from the specimens using a Reichert-Jung Ultracut E microtome, and the associated morphology was imaged using a JEOL 200CX transmission electron microscope at an accelerating voltage of 120 KV. Two different magnifications, 50k and 200 k, were used for the observations, and the respective results are shown in Figs. 2(a) and 2 (b). At low magnification, it was found that in some regions the clay is aggregated in the form of cluster structures. However, in other regions, no distinct clay platelets are observed. The micrographic observations indicate that the platelets are not dispersed and distributed homogeneously in the nanocomposites. According to the higher magnification micrographics, the interlayer spacing of the organoclay was estimated at 5 nm as indicated by the arrows in Fig. 2(b). Moreover, few exfoliated organoclay layers were found individually in the nanocomposites. Thus, XRD measurements and TEM observations suggest that the present samples could be regarded as intercalated nanocomposites. It should be noted that from XRD curves and TEM photographs, the morphology of the samples, as well as the extent of exfoliation, is not the same as those obtained by other researchers (Liu *et al*., 2004b; Zerda and Lesser, 2001; Mohan *et al*., 2006; Liu *et al*., 2005a)

IV. TENSILE TESTS OF EPOXY/ ORGANOCLAY NANOCOMPOSITES

To determine the organoclay effect on the mechanical properties of epoxy resin, nanocomposites were tested in tension. Coupon specimens as shown in Fig. 3 were fabricated from the pre-designed mold with Teflon-coated surface and then employed for tensile tests. The experiments were conducted on a hydraulic MTS machine with stroke control at a strain rate of 10^{-4} 1/s. Back-to-back strain gauges were mounted on the center of the specimens to eliminate the possible bending effect and to record the strain history during the tensile tests. The corresponding stress histories were obtained from the load cell embedded on the loading fixture.

Figure 4 illustrates the stress and strain curves for the pure epoxy and organoclay/epoxy material systems. Young's moduli of the samples obtained from Fig. 4 are summarized in Table 1. It was revealed that stiffness increases along with the increase of the organoclay loadings. The increases for organoclay nanocomposites have also been observed by other researchers (Mohan *et al*., 2006; Miyagawa *et al*., 2005; Balakrishnan and Raghavan, 2004; Miyagawa *et al*., 2004), and may be explained simply by the rule of mixture. However, the corresponding failure strains

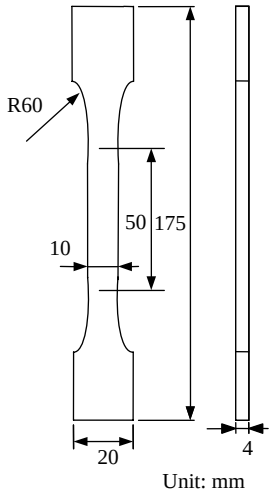

Fig. 3 Specimen configurations for tensile tests (unit: mm)

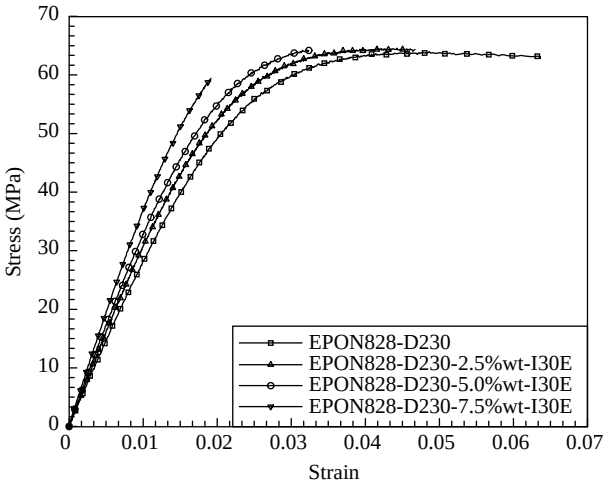

Fig. 4 Stress and strain curves for neat epoxy and nanocomposites with three different loadings of organoclay

decrease when the organoclay loadings increase. These phenomena imply that the inclusion of organoclay may enhance the stiffness of the epoxy resins but sacrifice their corresponding ductility. The declining tendency was also consistent with other organoclay/epoxy systems synthesized by mechanical shear mixing (Mohan *et al*., 2006).

V. FRACTURE PROPERTIES OF EPOXY/ ORGANOCLAY NANOCOMPOSITES

In the tensile tests mentioned above, the nanocomposites demonstrate higher stiffness but low ductility. To further investigate the effect of the organoclay on the Mode I fracture toughness (K_{IC}) of the nanocomposites and their fracture behaviors, the single-edge-notch bending (SENB) specimens were fabricated and then employed for the three-point-bending tests. The experiments were conducted basically following ASTM D5045 standards.

Table 1 Young's modulus of epoxy nanocomposites with different organoclay loadings

Materials	Young's modulus (GPa)	Enhancement ratio
Epoxy resin	3.0	
Nanocomposites (2.5wt% organoclay)	3.3	11%
Nanocomposites (5.0wt% organoclay)	3.5	18%
Nanocomposites (7.5wt% organoclay)	3.9	29%

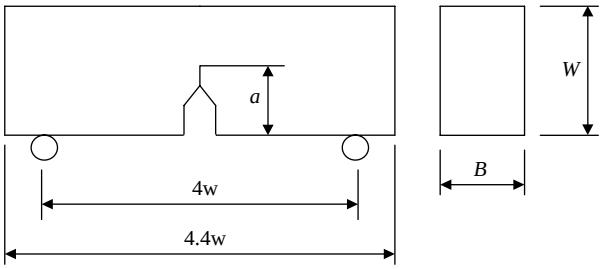

Fig. 5 SENB specimens for mode I fracture tests

The dimensions of the SENB specimens are illustrated in Fig. 5 where *B* denotes the thickness and *W* denotes the width of the sample. The pre-crack length (a in Fig. 5) was created by a jewel saw followed by a new razor blade in order to produce a sharp pre-crack tip. The correlations of the dimensions $W = 2B$ and $a = B$, suggested by ASTM D5045, were followed during the preparations of SENB specimens with the thickness *B* being around 6.2 mm. It is noted that in order to obtain a valid fracture toughness, the following inequality equation for the specimen size must be also satisfied

$$B,\ a,\ (W - a) > 2.5\ (K_I/\sigma_y)^2, \qquad (1)$$

where σ_y is the yielding stress of the materials which was determined using the offset method with 0.002 offset strains in the stress strain curves shown in Fig. 4. The detail dimensions for all tested SENB specimens associated with different organoclay loadings are summarized in Tables 2-5, respectively. It is noted that for each organoclay loading, at least four specimens were tested for the measurement of fracture toughness.

From the three point-bending-tests, the fracture toughness of SENB samples can be calculated using the following formulation:

Table 2 Fracture toughness for neat epoxy

	Thickness (B) (mm)	Width (W) (mm)	Crack length (a) (mm)	Fracture load (N)	Fracture toughness (K_{IC}) (MPa $m^{1/2}$)
Test1	6.24	12.43	6.5	76.13	1.29
Test2	6.24	12.4	6.15	109.18	1.65
Test3	6.22	12.36	6.15	94.96	1.45
Test4	6.23	12.36	6.15	84.07	1.28

Table 3 Fracture toughness for nanocomposites with 2.5 wt% organoclay

	Thickness (B) (mm)	Width (W) (mm)	Crack length (a) (mm)	Fracture load (N)	Fracture toughness (K_{IC}) (MPa $m^{1/2}$)
Test1	6.62	13.28	6.2	72.49	0.91
Test2	6.67	13.31	5.8	91.62	1.04
Test3	6.68	13.25	6.0	78.87	0.94
Test4	6.66	13.28	6.0	78.28	0.93

Table 4 Fracture toughness for nanocomposites with 5 wt% organoclay

	Thickness (B) (mm)	Width (W) (mm)	Crack length (a) (mm)	Fracture load (N)	Fracture toughness (K_{IC}) (MPa $m^{1/2}$)
Test1	6.09	11.70	5.75	51.74	0.80
Test2	6.01	12.10	5.7	51.30	0.75
Test3	5.98	12.07	5.7	57.78	0.85
Test4	6.02	12.12	5.8	50.42	0.75
Test5	6.04	11.77	5.4	54.15	0.77

Table 5 Fracture toughness for nanocomposites with 7.5 wt% organoclay

	Thickness (B) (mm)	Width (W) (mm)	Crack length (a) (mm)	Fracture load (N)	Fracture toughness (K_{IC}) (MPa $m^{1/2}$)
Test1	6.40	12.84	5.70	68.27	0.84
Test2	6.41	12.82	5.60	70.53	0.85
Test3	6.42	12.81	6.2	58.86	0.82
Test4	6.43	12.80	5.60	65.13	0.78

$$K_I = \frac{P_I}{B\sqrt{W}} f(x)$$

$$f(x) = 6x^{0.5}\frac{[1.99 - x(1-x)(2.15 - 3.93x + 2.7x^2]}{(1+2x)(1-x)^{3/2}}, \quad (2)$$

where P_I indicates the peak load in the load and deflection curves and x is a dimensionless value equal to the pre-crack length, a, divided by the sample width, W. The fracture tests were carried out on the servo-electrical control machine (HT-2102BP) at a displacement rate of 0.05 mm/min. The typical force versus displacement curves for the nanocomposites containing 5 wt% organoclay obtained from the three-point bending tests are shown in Fig. 6. It was found that the experimental data are quite linear during the loading process and then drop suddenly when the crack initiates. The peak value of the force was regarded as the failure load, P_I, and employed in the calculation of the fracture toughness given by Eq. (2). Fig. 7 illustrates the variations of fracture toughness of nanocomposites with different organoclay loadings. Apparently, fracture toughness of the nanocomposites decreases considerably with the addition of the organoclay. Furthermore, the reduction tendency is not significant as the organoclay loadings are greater than 5 wt%.

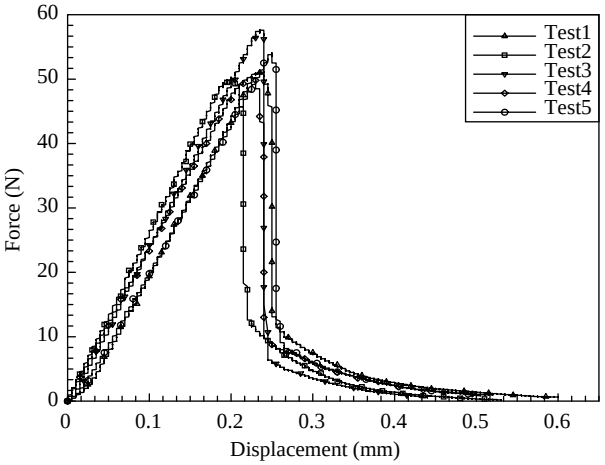

Fig. 6 Displacement and force curves for nanocomposites with 5 wt% organoclay loading in three-point-bending test

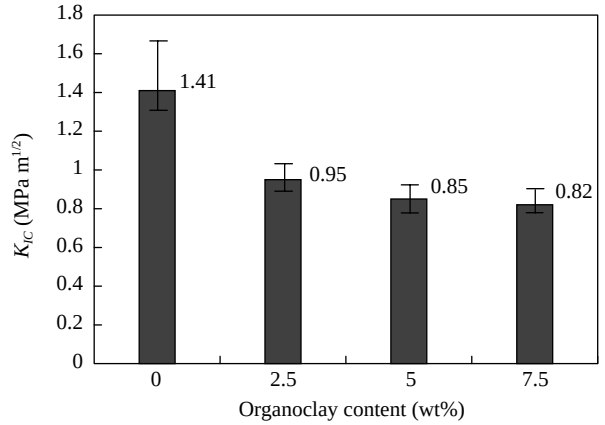

Fig. 7 Fracture toughness of the nanocomposites with different organoclay loadings

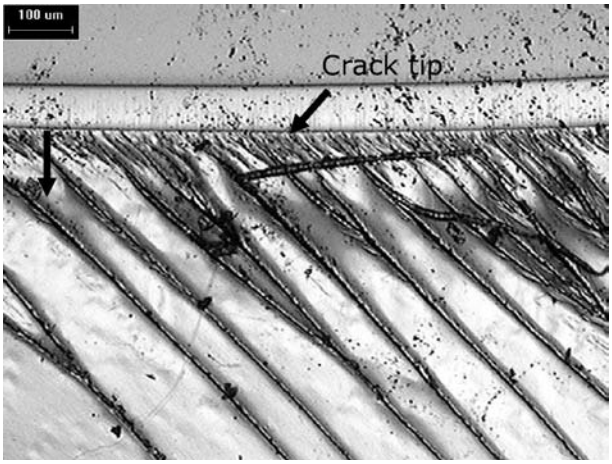

Fig. 8 Optical microscope photo of neat epoxy in fracture tests (50 magnification)

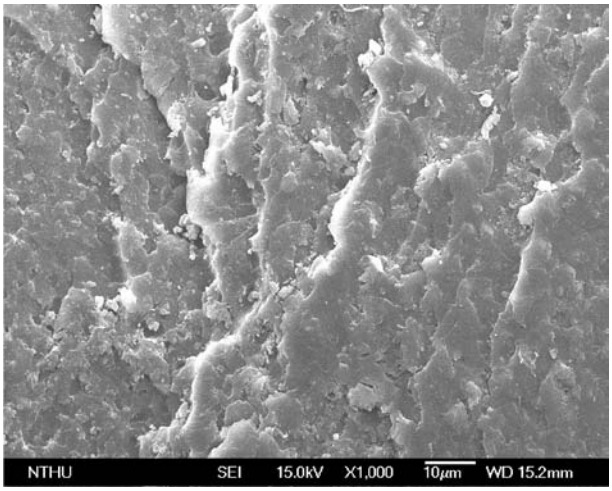

Fig. 9 SEM photomicrographs of nanocomposites with 2.5 wt% organoclay in fracture test (1000 magnification)

These phenomena could be attributed to two things. One is that the plastic deformation around the crack tip is constrained by the organoclay within the nanocomposites such that a sudden brittle fracture could take place. The other might be the poor interface adhesion between the organoclay and epoxy resin in the nanocomposites resulting in an easily initiated crack.

In order to investigate the decreasing fracture toughness of nanocomposites, the failure surfaces of the specimens around the crack tips were examined using optical microscopy and SEM. Fig. 8 show the fracture surfaces of the pure epoxy obtained using an optical microscope. The arrows pointing downward in the figures indicate the cracks' propagation direction. It was shown that significant river-type marks near the crack tip were found indicating the typical fractography of brittle failure behavior (Liu *et al.*, 2004b). The fracture surfaces of the nanocomposites with 2.5, 5, 7.5 wt% loading of organoclay were examined using SEM, and the results are shown in Figs. 9-11. It is interesting to note that for the nanocomposites, obvious scale-like patterns are present on the failure surfaces, which deviate from the failure mechanism of pure epoxy samples. This could be responsible for the great drop in fracture toughness in the transition from pure epoxy to nanocomposites. The formation of the scale-like patterns may be due to the nodular microstructures of epoxy caused by the presence of organoclay platelets. In addition, the interfacial debonding between the organoclay and epoxy or interlayer delamination within the platelet could also result in the scale-like failure marks and thereafter diminish the fracture toughness of the nanocomposites. It should be noted that the scale-like failure pattern is different from the microvoids failure mechanism observed in other

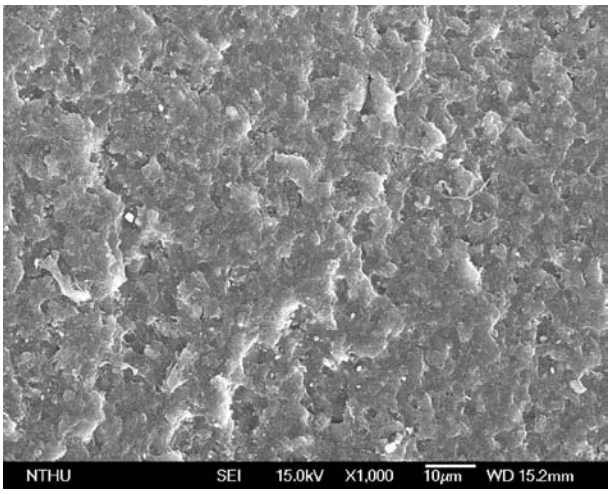

Fig. 10 SEM photomicrographs of nanocomposites with 5 wt% organoclay in fracture test (1000 magnification)

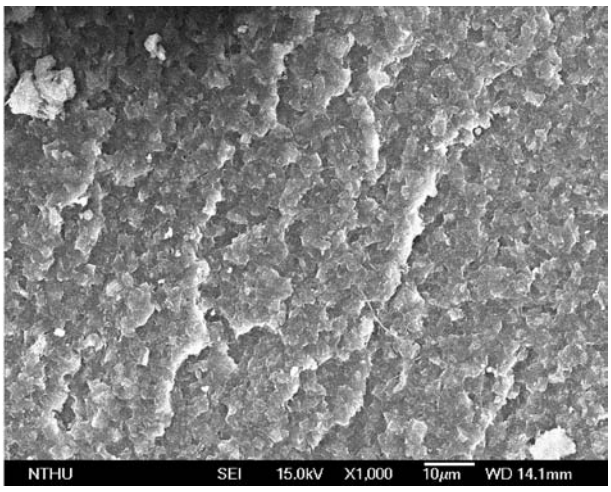

Fig. 11 SEM photomicrographs of nanocomposites with 7.5 wt% organoclay in fracture test (1000 magnification).

material systems (Liu *et al*., 2004b; Liu *et al*., 2005a; Liu *et al*., 2005b) and the organoclay effect on the fracture toughness is also dissimilar accordingly. Therefore, to fully understand the failure mechanism, it is necessary to invoke molecular simulations on the study of the morphologies of the nanocomposites as well as the interaction between the polymer and organoclay platelets.

VI. CONCLUSIONS

Intercalated nanocomposites with three different organoclay loadings were fabricated using sonication. The spacing between the adjacent platelets is around 5 nm. Tensile tests indicate that Young's modulus of the nanocomposites increases with the increment of the organoclay; however, the corresponding failure strain decreases as the amount of organoclay loading increases. In addition, Mode I fracture tests show that the fracture toughness of nanocomposites decreases as organoclay loading increases. SEM observations demonstrate scale-like marks on the failure surfaces of nanocomposites, which are different from those on pure epoxy resin. The discrepancy is believed to be the result of the changes of morphology of epoxy resin due to the presence of organoclay. Therefore, organoclay not only influences the morphology of the epoxy resin but also alters the corresponding failure mechanism. To fully understand the organoclay effect on fracture toughness, it is necessary to study the interaction of organoclay and epoxy using a molecular mechanics approach.

ACKNOWLEDGEMENTS

This research was supported by the National Science Council, Taiwan, under the contract No. NSC 94-2212-E-009-017 to National Chiao Tung University.

REFERENCES

Balakrishnan, S., and Raghavan, D., 2004, "Acrylic, Elastomeric, Particle-Dispersed Epoxy-Clay Hybrid Nanocomposites: Mechanical Properties," *Macromolecular Rapid Communications*, Vol. 25, No. 3, pp. 481-485.

Cho, J. W., and Paul, D.R., 2001, "Nylon 6 Nanocomposites by Melt Compounding," *Polymer*, Vol. 42, No. 3, pp. 1083-1094.

Dennis, H. R., Hunter, D. L., Chang, D., Kim, S., White, J. L., Cho, J. W., and Paul, D. R., 2001, "Effect of Melt Processing Conditions on the Extent of Exfoliation in Organoclay-Based Nanocomposites," *Polymer*, Vol. 42, No. 23, pp. 9513-9522.

Gam, K. T., Miyamoto, M., Nishimura, R., and Sue, H. J., 2003, "Fracture Behavior of Core-Shell Rubber-Modified Clay-Epoxy Nanocomposites," *Polymer Engineering and Science*, Vol. 43, No. 10, pp. 1635-1645.

LeBaron, P. C., Wang, Z., and Pinnavaia, T. J., 1999, "Polymer-Layered Silicate Nanocomposites: An Overview," *Applied Clay Science*, Vol. 15, No. 1, pp. 11-29.

Liu, T., Tjiu, W. C., Tong, Y., He, C., Goh, S. S., and Chung, T. S., 2004b, "Morphology and Fracture Behavior of Intercalated Epoxy/Clay Nanocomposites," *Journal of Applied Polymer Science*, Vol. 94, No. 3, pp. 1236-1244.

Liu, W., Hoa, S. V., and Pugh, M., 2004a, "Morphology and Performance of Epoxy Nanocomposites

Modified with Organoclay and Rubber," *Polymer Engineering and Science*, Vol. 44, No. 6, pp. 1178-1186.

Liu, W., Hoa, S. V., and Pugh, M., 2005a, "Fracture Toughness and Water Uptake of High-Performance Epoxy/Nanoclay Nanocomposites," *Composites Science and Technology*, Vol. 65, No. 15-16, pp. 2364-2373.

Liu, W., Hoa, S. V., and Pugh, M., 2005b, "Organoclay-Modified High Performance Epoxy Nanocomposites," *Composites Science and Technology*, Vol. 65, No.2, pp. 307-316.

Lu, H., Roy, S., Sampathkumar, P. and Ma, J., 2002, "Characterization of the Fracture Behavior of Epoxy Nanocomposites." *Proceedings of the American Society for Composites*, 17th Technical Conference, West Lafayette, IN, USA.

Miyagawa, H., and Drzal, L.T., 2003, "Fracture Behavior of Epoxy/Clay and Epoxy/Silica nanocomposites", *Proceeding of the 14th International Conference on Composite Materials (ICCM-14)*, CA, USA.

Miyagawa, H., Foo, K. H., Daniel, I. M., and Drzal, L. T., 2005, "Mechanical Properties and Failure Surface Morphology of Amine-Cured Epoxy/Clay Nanocomposites," *Journal of Applied Polymer Science*, Vol. 96, No. 2, pp. 281-287.

Miyagawa, H., Rich, M. J., and Drzal, L. T., 2004, "Amine-Cured Epoxy/Clay Nano-composites. II. the Effect of the Nanoclay Aspect Ratio," *Journal of Polymer Science Part B-Polymer Physics*, Vol. 42, No. 23, pp. 4391-4400.

Mohan, T. P., Kumar, M. R., and Velmurugan, R., 2006, "Thermal, Mechanical and Vibration Characteristics of Epoxy-Clay Nanocomposites," *Journal of Materials Science*, Vol. 41, No. 18, pp. 5915-5925.

Nair, S. V., Goettler, L. A., and Lysek, B. A., 2002, "Toughness of Nanoscale and Multiscale Polyamide-6,6 Composites," *Polymer Engineering and Science*, Vol. 42, No. 9, pp. 1872-1882.

Okada, A., and Usuki, A., 1995, "The Chemistry of Polymer-Clay Hybrids," *Materials Science and Engineering C*, Vol. 3, No. 2, pp. 109-115.

Pinnavaia, T. J., and Beall, G. W., 2000, Polymer-Clay Nanocomposites, John Wiley & Sons Ltd, NY, USA.

Technical data sheet, *Nanocor Inc*.

Thostenson, E. T., Li, C., and Chou, T.W., 2005, "Nanocomposites in context," *Composites Science and Technology*, Vol. 65, No. 3-4, pp. 491-516.

Usuki, A., Kawasumi, M., Kojima, Y., Okada, A., Kurauchi, T., and Kamigaito, O., 1993a, "Swelling Behavior of Montmorillonite Cation Exchanged for ω-amino Acids by ε-Caprolactam," *Journal of Materials Research*, Vol. 8, No. 5, pp. 1174-1178.

Usuki, A., Kojima, Y., kawasumi, M., Okada, A., Fukushima, Y., Kurauchi, T., and Kamigaito, O., 1993b, "Synthesis of Nylon 6-Clay Hybrid," *Journal of Materials Research*, Vol. 8, No. 5, pp. 1179-1184.

Wang, W., Wu, J., Chen, L., He, C., and Toh, M., 2004, "Mechanical Properties and Fracture Behavior of Epoxy Nanocomposites with Highly Exfoliated Pristine Clay", *ANTEC*, Vol. 2, pp. 1820-1824.

Zerda, A. S., and Lesser, A. J., 2001, "Intercalated Clay Nanocomposites: Morphology, Mechanics, and Fracture Behavior," *Journal of Polymer Science Part B: Polymer Physics*, Vol. 39, No. 11, pp. 1137-1146.

Manuscript Received: Jan. 05, 2007
Revision Received: June 08, 2007
and Accepted: June 25, 2007